



OPEN ACCESS

EDITED BY

Yuanjian Fang,
Zhejiang University, China

REVIEWED BY

Marion Mussbacher,
University of Graz, Austria
Andrea Emilse Errasti,
University of Buenos Aires, Argentina
Ningbo Xu,
Southern Medical University, China
Yingkun He,
Henan Provincial People's Hospital, China

*CORRESPONDENCE

Bing Zhao

✉ drzhaobing@yahoo.com

Hua Yang

✉ yhmed@163.com

†These authors have contributed
equally to this work

RECEIVED 04 February 2023

ACCEPTED 27 April 2023

PUBLISHED 08 May 2023

CITATION

Han Y, Li G, Zhang Z, Zhang X, Zhao B
and Yang H (2023) Axl promotes
intracranial aneurysm rupture by
regulating macrophage polarization
toward M1 via STAT1/HIF-1 α .
Front. Immunol. 14:1158758.
doi: 10.3389/fimmu.2023.1158758

COPYRIGHT

© 2023 Han, Li, Zhang, Zhang, Zhao B
and Yang. This is an open-access article
distributed under the terms of the [Creative
Commons Attribution License \(CC BY\)](#). The
use, distribution or reproduction in other
forums is permitted, provided the original
author(s) and the copyright owner(s) are
credited and that the original publication in
this journal is cited, in accordance with
accepted academic practice. No use,
distribution or reproduction is permitted
which does not comply with these terms.

Axl promotes intracranial aneurysm rupture by regulating macrophage polarization toward M1 via STAT1/HIF-1 α

Yongquan Han^{1,2†}, Gaozhi Li^{2†}, Zeyu Zhang², Xiaohua Zhang²,
Bing Zhao^{2*} and Hua Yang^{1*}

¹Department of Neurosurgery, the Affiliated Hospital of Guizhou Medical University, Guiyang, China,

²Department of Neurosurgery, Renji Hospital, Shanghai Jiaotong University School of Medicine, Shanghai, China

Background: Macrophage infiltration and polarization are crucial for the pathogenesis of intracranial aneurysm (IA) rupture. Axl, a receptor tyrosine kinase, is involved in inflammation and efferocytosis in multiple organs. Upregulated soluble Axl in cerebrospinal fluid (CSF) and plasma is correlated with intracranial aneurysm rupture. This study aimed to investigate the role of Axl in IA rupture and macrophage polarization.

Methods: Male C57BL/6J mice were used to induce IA. The level of Axl from control vessels and unruptured and ruptured IA samples was detected. In addition, the relationship between Axl and macrophages was confirmed. The pathway of Axl-mediated macrophage polarization was explored after IA induction *in vivo* and in bone marrow-derived macrophages (BMDMs) stimulated by LPS/IFN- γ *in vitro*. The animals were randomized into three groups and treated intraperitoneally with the vehicle, selective AXL antagonist R428, and recombinant mouse growth arrest-specific 6 (rmGas6) for 21 consecutive days. Then, we evaluated the influence of Axl on IA rupture by administrating R428 to inhibit or rmGas6 to activate the Axl receptor *in vivo*.

Results: Compared with that in normal vessels, Axl expression was significantly upregulated in unruptured IA samples. The ruptured IA tissue exhibited significantly higher expression of Axl than the unruptured IA tissue. Axl and F4/80 were coexpressed in IA tissue and LPS/IFN- γ -stimulated BMDMs. R428 treatment significantly reduced the rate of M1-like macrophage infiltration and IA rupture. In contrast, rmGas6 treatment promoted M1 macrophage infiltration and IA rupture. Mechanistically, R428 inhibited the phosphorylation of Axl and STAT1 and the expression of hypoxia-inducible factor-1 α (HIF-1 α) and decreased the levels of IL-1 β , NOS2, and MMP9 in LPS/IFN- γ -stimulated BMDMs. rmGas6 promoted the phosphorylation of Axl and STAT1 and the expression of HIF-1 α . In addition, STAT1 knockdown abolished Axl-mediated M1 macrophage polarization.

Conclusion: The inhibition of Axl reduced macrophage polarization toward the M1 phenotype *via* the STAT1/HIF-1 α signaling pathway and prevented IA rupture in mice. This finding suggests that pharmacological inhibition of Axl might be used to prevent the progression and rupture of IA.

KEYWORDS

intracranial aneurysm, rupture, Axl, macrophage polarization, STAT1, HIF-1 α

Introduction

The prevalence of unruptured intracranial aneurysm (IA) is estimated to be approximately 3.2% in the population around the world (1). Unruptured IAs are more frequently detected with the modern imaging modalities used in clinical practice. Ruptured IAs have a high rate of mortality and morbidity and cause a lifelong cognitive deficit for those who survive (2, 3). Most IAs are found incidentally and need preventive treatment to prevent rupture. Currently, there are two main treatment modalities, clipping and coiling, which are associated with high procedure-related complications (4). Therefore, pharmacological therapy may be a potential way to prevent IA rupture with minimal risk (5, 6).

IA is associated with complicated pathological changes characterized by an inflammatory response triggered by abnormal hemodynamic stresses in cerebral arteries (7–9). Recent studies have shown that the infiltration of the proinflammatory macrophage subtype, classified as M1-like macrophages, can exacerbate pathogenesis and promote IA rupture (10, 11). Macrophage-mediated cellular and molecular inflammation are crucial in aneurysm rupture.

A family of receptor tyrosine kinases, Tyro3, Axl, and Mer (TAM), expressed on macrophages, mediates the process of efferocytosis, phagocytosis, and the inflammatory response (12–15). In contrast to Tyro3 and Mer, the expression of Axl is stimulated by proinflammatory mediators in macrophages and dendritic cells (16, 17). In addition, the extracellular domain of Axl is proteolytically cleaved and released, which is called soluble Axl (solAxl). The upregulated solAxl in both cerebrospinal fluid (CSF) and plasma is correlated with IA rupture (18). However, whether Axl regulates the macrophage response in aneurysm biopsies in a manner that causes IA rupture needs to be investigated. Moreover, the detailed mechanism of Axl in the process and pathogenesis of IA is still unclear.

To clarify the role of Axl in IA rupture, we evaluated Axl expression and its relationship with macrophage infiltration in mouse IA models. We further determined whether Axl promotes macrophage polarization toward the M1 phenotype by activating STAT1/HIF-1 α signaling, which promotes aneurysm rupture. This study potentially provides a new therapeutic target and may facilitate the design of pharmacological treatments for IAs.

Materials and methods

The induction of the mouse IA model

Animal experimental protocols were approved by the Institutional Animal Care and Use Committee of Shanghai Jiaotong University. Male C56BL/6J mice (6–8 weeks) were purchased from Charles River Laboratories (Shanghai, China). IA was induced by combining systemic hypertension and elastase injection as previously described (19). Briefly, after being anesthetized by a mixture of 3% isoflurane and O₂ (1 L/min) on a heating pad, individual mice were subjected to ligation of the left common carotid artery and bilateral posterior branches of the renal artery with 6-0 nylon suture. One week later, the mice were anesthetized as described above and fixed in a stereotaxic frame with a mouse adaptor (RWD, China). According to the coordinates from Mouse Brain Atlas, mice were injected with 35 mU (milli-unit) elastase (E1250, Sigma-Aldrich, USA) through a Hamilton syringe with a 34 G needle (Hamilton, Switzerland) at a rate of 0.2 μ l/min into their suitable basal cistern (2.5 mm posterior to the bregma, 1.0 mm right to the middle and 5.3 mm deep to the skull surface). Subsequently, an osmotic pump (A1004, Alzet Osmotic Pump, USA) containing angiotensin II (A1042, APEX BIO, USA) was implanted into a subcutaneous pocket between the scapulae to deliver angiotensin II at a rate of 1000 ng/kg/min for systemic hypertension induction. Upon recovery, the mice were fed food containing 8% NaCl and 0.12% BAPN (N-methyl- β -alanine nitrile, M27603, Sigma-Aldrich, USA).

Animal treatment

To investigate the effect of Axl on IA rupture, we administered the selective AXL antagonist R428 and recombinant mouse growth arrest-specific 6 (rmGas6) *in vivo* to inhibit or activate the biological effect of Axl, respectively. Mice that died within 7 days after IA induction were excluded. One week later, the animals were randomized into three groups (n=15 each group) and treated intraperitoneally with vehicle (phosphate-buffered saline, PBS), 75 mg/kg R428 (HY-15150, MCE, USA) or 4 μ g/kg rmGas6 (986-GS, R&D Systems, USA) every day for 21 consecutive days. The concentration of R428 administered intraperitoneally was 2 mmol/L. The doses of R428 and rmGas6

were applied according to previous studies (20, 21). Systolic arterial blood pressure (SBP) was measured and recorded from IA induction with tail-cuff measurement (Softron, BP-2010, Japan). All animals were euthanized for tissue harvest 21 days after IA induction.

Tissue harvest

The mice were monitored daily. Intracranial aneurysm formation was defined as localized outward bulging of the artery wall. After euthanization, the mice were perfused with precooled PBS, 4% paraformaldehyde, and Microfil (MV-120, Flow Tech, USA) sequentially to visualize vessels under a microscope by two researchers in a blinded manner. Intracranial aneurysms were classified as follows: Grade 0, normal artery; Grade 1, artery dilation or tortuosity; Grade 2, unruptured aneurysm; and Grade 3, ruptured aneurysm. Unruptured aneurysms were defined as 1.5 times larger in diameter than the parent artery. An aneurysm with fresh blood clots along the cerebral artery, revealing subarachnoid hemorrhage, was defined as aneurysm rupture.

Preparation of bone marrow-derived macrophages

Bilateral femurs and tibiae were dissected from male C57BL/6J mice and flushed with sterilized PBS. After lysis of red blood cells with Red Blood Cell Lysis Buffer (11814389001, Roche, Switzerland), the remaining nuclear cells were filtered through a 70 μm cell strainer (352350, Corning, USA). BMDMs were diluted to 5×10^5 cells per milliliter and cultured in Dulbecco's modified Eagle's medium (DMEM) containing 10% FBS and 1% penicillin/streptomycin in the presence of 25 ng/ml recombinant murine M-CSF (315-02, Peprotech, USA) for 7 days to induce macrophage maturation at 37°C in a 5% CO₂ incubator.

Cell transfection

Cells extracted from bone marrow were small round cells and were plated in a culture dish at a concentration of 5×10^5 cells/ml and incubated with M-CSF stimulation for 7 days. During stimulation with M-CSF, BMDMs became larger with different-shaped antennae. The cell volume reached 70% of the dish area after 7 days of stimulation with M-CSF. Cells were transfected with 100 nM control scramble (6568, CST, USA) or 100 nM STAT1 siRNA (sc-44124, Santa Cruz, USA) using Lipofectamine™ 3000 (L3000001, Invitrogen, USA) according to the manufacturers' instructions. The transfection efficiency was evaluated by real-time quantitative PCR (RT-qPCR) and Western blotting.

Induction of M1 macrophage polarization

Mouse BMDMs were cultured in serum-free medium for 6 hours and treated with 100 ng/ml LPS and 20 ng/ml IFN- γ (HY-

D1056/HY-P7071, MCE, USA) for 6 hours in complete medium containing 1 $\mu\text{g/ml}$ R428 and 200 ng/ml rmGas6 to inhibit or enhance the phosphorylation of Axl.

Human acute monocytic leukemia THP-1 cells were purchased from Procell (Wuhan, China). THP-1 cells were cultured in RPMI-1640 medium containing 10% (v:v) fetal bovine serum and 1% (v:v) penicillin-streptomycin solution. THP-1 cells were differentiated into macrophages by incubation with 0.5 μM 12-O-tetradecanoylphorbol 13-acetate/PMA (A606759, Sangon Biotech, China) for 12 hours. After washing with PBS, the THP-1 macrophages were primed with 100 ng/ml LPS and 20 ng/ml IFN- γ to polarize toward M1 macrophages and treated with or without R428 and Gas6 (HY-P77668, MCE, US) for 6 hours.

Hematoxylin and eosin and Masson's trichrome staining

Individual tissue samples were fixed in 4% paraformaldehyde overnight. Then, the tissue samples were processed, paraffin-embedded, and sectioned manually, as described previously. The tissue sections (10 μm) were stained with HE (G1120, Solarbio, China) and Masson (G1340, Solarbio, China) according to the manufacturers' instructions.

Immunofluorescence

The fixed vascular tissues were dissected and frozen in OCT compound. The crystal tissue sections (10 μm) were cultured with 0.3% Tween-100 for 30 min and blocked with 5% donkey serum for 1 h at room temperature. Similarly, the coating coverslips (WHB-12-CS, WHB Scientific, China) on which cells were plated were fixed and treated as described above. These samples were incubated overnight at 4°C with primary antibodies against Axl (13196, Proteintech), CD86 (14-0862-82, Invitrogen, USA), pSTAT1 (9167, Abcam) and F4/80 (71299, CST). After being washed with PBS, the slides were exposed to the indicated fluorophore-labeled secondary antibodies (ab150075, ab150165, Abcam, USA) at room temperature for 2 hours and nuclear-stained 4',6-diamidino-2-phenylindole (DAPI) (C1002, Beyotime, China). The fluorescent signals were examined and photo imaged under a laser scanning confocal microscope (LSM800, Zeiss, Germany).

Quantitative real-time -PCR

Total RNA was extracted from individual cell samples and purified using an RNA extraction kit (AG21017, Accurate Biology, China) according to the manufacturers' instructions. After RNA concentration quantitation through a spectrophotometer (ND-1000, Nanodrop Technologies, USA), RNA samples were individually reverse-transcribed into cDNA using PrimeScript™ RT Master Mix (RR036A, Takara, Japan). The relative levels of targeted gene mRNA transcripts to the control GAPDH were quantified by TB Green® Premix Ex Taq™ II (RR820, Takara,

Japan) and specific primers in a Real-Time PCR System (StepOne Plus, Thermo, USA). The PCRs were performed in duplicate, and the data were analyzed by the $2^{-\Delta\Delta C_t}$ method. The primer sequences are listed below.

Axl (Forward: TGA GCC AAC CGT GGA AAG AG; Reverse: AGG CCA CCT TAT GCC GAT CTA)

Il-1 β (Forward: CAC TAC AGG CTC CGA GAT GAA CAA C; Reverse: TGT CGT TGC TTG GTT CTC CTT GTA C)

Nos2 (Forward: AGC GAG GAG CAG GTG GAA; Reverse: GGA AAA GAC TGC ACC GAA GAT ATC)

Mmp9 (Forward: GTA CTC GAC CTG TAC CAG CG; Reverse: TCA GGG CGA GGA CCA TAG AG)

Gapdh (Forward: GGG GAG CGA GAT CCC TCC AAA ATC AAG TGG GG; Reverse: GGG TCA TGA GTC CTT CCA CGA TAC CAA AGT TG).

Western blot

The different groups of cells were lysed with radioimmunoprecipitation assay (RIPA) buffer (P0013, Beyotime, China) with a dose of 100 μ l RIPA per 1×10^6 cells. After being boiled with sample buffer at 99°C for 5–10 mins, the cell lysates were separated by SDS-PAGE and transferred to PVDF membranes. After being blocked with 5% nonfat milk dissolved in TBST, the membranes were incubated at 4°C overnight with primary antibodies against Axl (bs-5180R, Bioss, China), pAxl (bs-5181R, Bioss, China), STAT1 (14994S, CST, USA), pSTAT1 (7649S, CST, USA), HIF-1 α (ab179483, Abcam, USA), IL-1 β (CY5087, Abways, China), NOS2 (CY5993, Abways, China), MMP9 (CY5205, Abways, China) and β -actin (81115, Proteintech, China). The membranes were exposed to the indicated HRP-conjugated secondary antibodies at room temperature for 1 hour and visualized with ECL through an imaging system (Tanon, China).

Statistical analysis

Continuous variables were reported as the mean \pm standard deviation and analyzed using GraphPad Software (v9.0.1). The continuous variants among multiple groups were compared by one-way ANOVA and *post hoc* test. The rates of aneurysm rupture in the different groups of mice are presented as frequencies or percentages and were analyzed with Fisher's exact test. The pathological grade data were converted into rank data and tested with the Kruskal-Wallis method. The systolic blood pressure data were analyzed with two-way ANOVA. The survival analysis was performed with the log-rank test. A P value of < 0.05 was considered statistically significant.

Results

IA was induced in mice

To explore the effect of Axl on the pathogenic process of IA, we established a mouse model of IA (Figure 1A). Of the 60 mice, 15 died

within 7 days after IA induction for unknown reasons after surgery and were excluded. Representative images of normal arteries, unruptured aneurysms, and ruptured aneurysms in the circle of Willis are shown in Figure 1B. To ascertain the pathological changes in IA, hematoxylin-eosin staining (HE) and Masson's trichrome staining were performed. Compared to normal vessels, HE staining showed thickening of the vascular media and disordered and scattered smooth muscle cells in unruptured aneurysms and thinning of the vessel wall in ruptured aneurysms (Figure 1C). Masson's trichrome staining revealed the disconnection of elastic fibers in the vessel of the aneurysm (Figure 1D).

Upregulated Axl expression was associated with M1 macrophage infiltration in aneurysm lesions

Immunofluorescence revealed upregulated Axl expression in unruptured aneurysms compared with normal arteries (34.5% vs. 3.9%, $P < 0.0001$) and ruptured aneurysms (53.0% vs. 34.5%, $P < 0.001$; Figures 2A, B). Simultaneously, the results also revealed an increase in CD86⁺ (a marker of M1 macrophages) cells in unruptured aneurysms compared with normal arteries (48.0% vs. 11.1%, $P < 0.0001$) and a further increase in ruptured aneurysms (78.8% vs. 48.0%, $P < 0.0001$; Figures 2C, D). Double immunofluorescence of IA tissue sections showed that Axl and F4/80 were colocalized in IA tissues (Figure 2E). Costaining of Axl and SM22 α is shown in Supplementary Figure S1.

Axl activation promoted M1-like macrophage polarization *in vitro*

To further explore the relationship between Axl expression and M1-like macrophage polarization, BMDMs and THP-1 cells were stimulated with or without LPS/IFN- γ (100/20 ng/ml) for 6 hours. LPS/IFN- γ stimulation induced *Axl* expression at the mRNA ($P < 0.05$, Figure 3A) and protein levels (Figures 3B, C). Axl colocalized with F4/80 in LPS/IFN- γ -stimulated BMDMs (Figure 3D). LPS/IFN- γ -primed THP-1 macrophages exhibited increased Gas6 ($P < 0.01$) and Axl ($P < 0.01$) expression and pAxl expression ($P < 0.0001$) (Supplementary Figure S2). BMDMs were treated with vehicle, R428 and rmGas6. Compared with the control treatment, R428 treatment inhibited *Il-1 β* ($P < 0.01$), *Nos2* ($P < 0.001$), and *Mmp9* ($P < 0.01$) mRNA expression in M1-like macrophages (Figures 3E–G). Conversely, rmGas6 treatment had the opposite effect on gene transcription in BMDMs (*Il-1 β* , $P < 0.0001$; *Nos2*, $P < 0.01$; *Mmp9*, $P < 0.0001$, Figures 3E–G). Consistent with the qRT-PCR results, Western blot analysis revealed that R428 treatment inhibited Axl phosphorylation and attenuated IL-1 β , NOS2, and MMP9 expression. rmGas6 promoted Axl phosphorylation, and increased IL-1 β , NOS2, and MMP9 in M1-like macrophages (Figures 3H–J).

LPS/IFN- γ -primed THP-1 cells were treated with vehicle, R428 and rGas6. R428 treatment showed a lower level of pAxl ($P < 0.01$), while the levels of Gas6 and Axl did not show a significant difference, and the secretion of IL-1 β was attenuated ($P < 0.01$). In

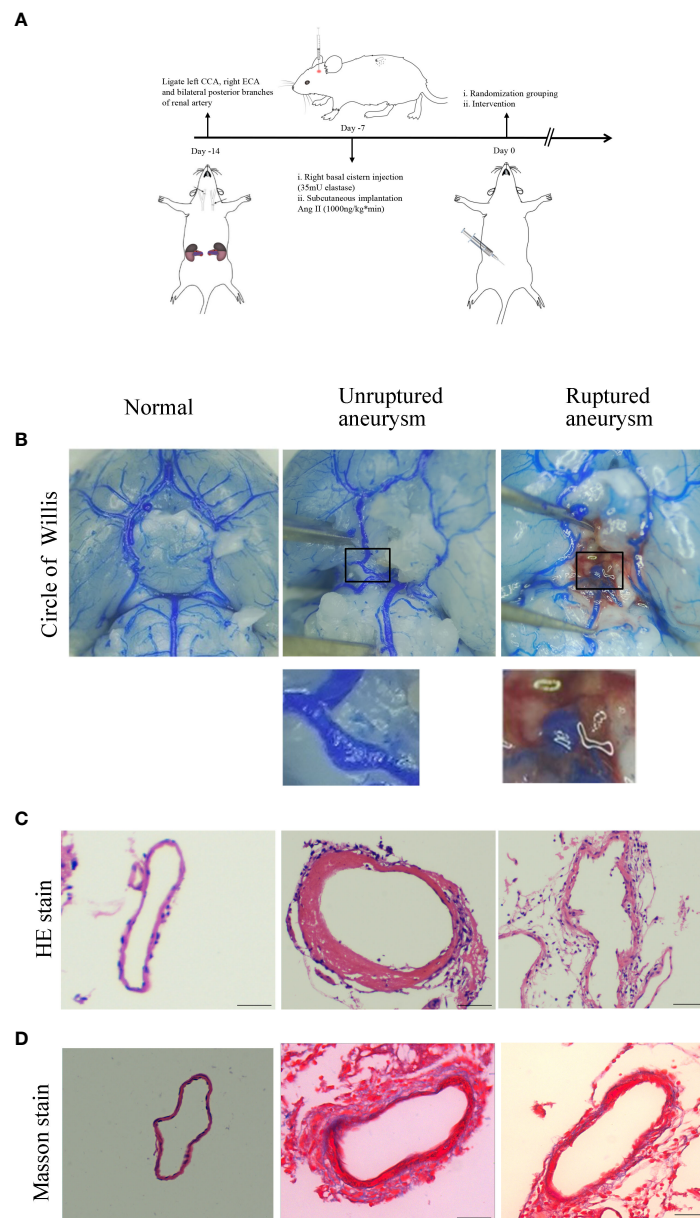


FIGURE 1

Intracranial aneurysm was established in mice. (A) Diagram of IA induction. (B) Representative images of normal artery, unruptured aneurysm, and ruptured aneurysm with subarachnoid hemorrhage. (C) Hematoxylin and eosin (H&E) staining showed scattered arranged cells in the mouse model of aneurysm. (D) Masson's trichrome staining showed the destruction of vessel walls in the aneurysm. Scale bars=50 μ m.

contrast, Gas6 treatment in LPS/IFN- γ -primed THP-1 cells enhanced pAxl ($P < 0.01$) and the secretion of IL-1 β ($P < 0.05$) without changing Axl. Gas6 plus R428 treatment inhibited pAxl ($P < 0.01$) and IL-1 β ($P < 0.01$) secretion, as shown in [Supplementary Figure S2](#).

STAT1 knockdown abolished the promoting effect of Axl on M1 polarization

We found that R428 treatment inhibited the phosphorylation of STAT1 and expression of HIF-1 α , while the phosphorylation of

STAT1 and level of HIF-1 α were promoted by rmGas6 in M1-like macrophages ([Figures 4A, B](#)). To illuminate the role of STAT1 in Axl-mediated macrophage polarization, the STAT1 level was knocked down *via* STAT1-specific siRNA, and the efficiency of knockdown was confirmed at the mRNA ($P < 0.01$) and protein levels ([Figures 4C, D](#)). Compared with the si-CTR group, STAT1 knockdown attenuated IL-1 β ($P < 0.001$), *Nos2* ($P < 0.05$), and *Mmp9* ($P < 0.0001$) in rmGas6-treated M1 macrophages ([Figures 4E–G](#)). Western blot analysis showed the same result, as well as HIF-1 α decline ([Figures 4H, I](#)). These results revealed that the effect of Axl on M1-like macrophage polarization was abolished by STAT1 knockdown.

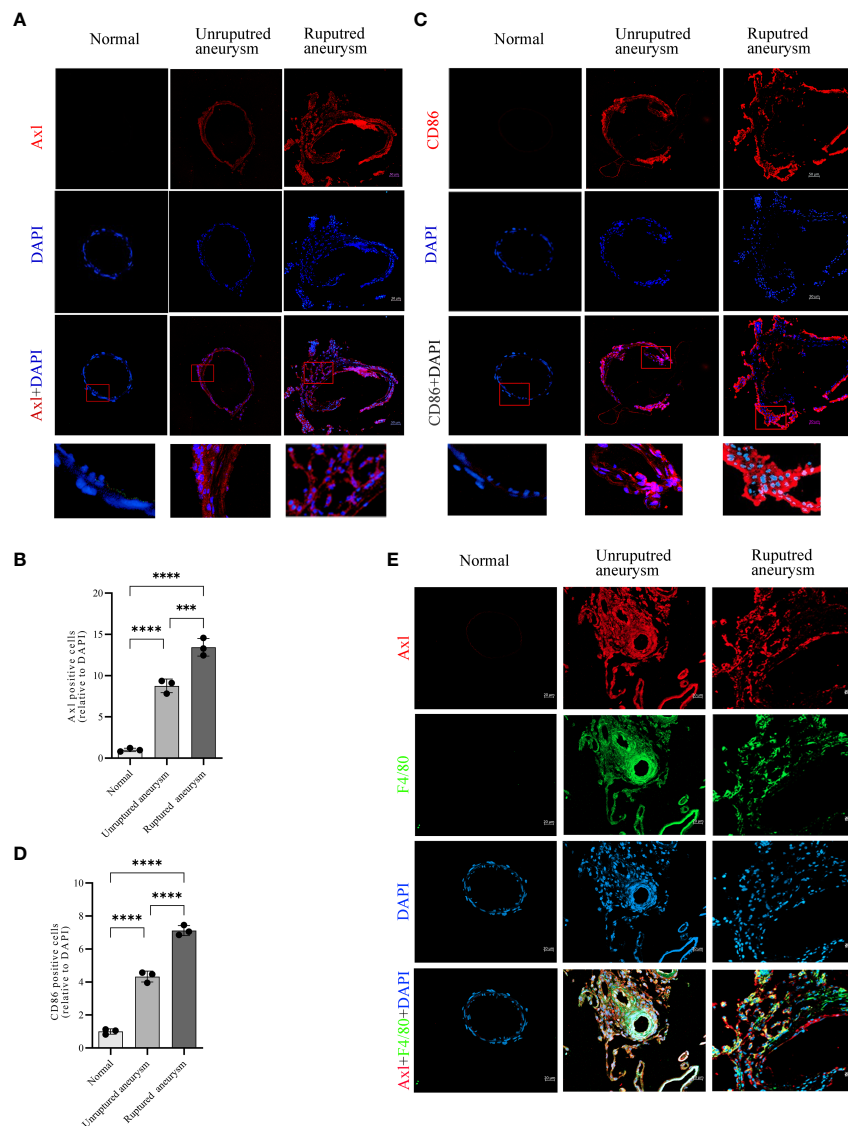


FIGURE 2

Increased expression of Axl and M1 macrophage infiltration in unruptured and ruptured aneurysm sections compared to normal cerebral artery. Representative immunofluorescence images of Axl (A) and CD86 (C) expression in normal arteries and unruptured and ruptured aneurysms. Quantitative analysis of Axl (B)- and CD86 (D)-positive cells. Scale bar = 20 μ m (E), Axl (red) and F4/80 (green) coexpressed in aneurysm walls. *** P <0.001, **** P <0.0001.

Activated Axl promotes intracranial aneurysm rupture in mice

IA mice were designed and treated with vehicle, R428, and rmGas6 in a flowchart (Figure 5A). Compared with vehicle treatment, R428 treatment inhibited the phosphorylation of STAT1 (39.0% vs. 30.8%, P <0.01. Figures 5B, C) and significantly decreased M1-like macrophage infiltration in aneurysm walls (44.7% vs. 24.7%, P <0.05. Figures 5D, E). However, rmGas6 treatment boosted the phosphorylation of STAT1 (51.6% vs. 39.0%, P <0.01. Figures 5B, C) and M1-like macrophage infiltration (44.7% vs. 73.0%, P <0.01. Figures 5D, E).

The analysis revealed different compositions of pathological grades among the three groups (R428 vs. vehicle, n =15, P <0.05; rmGas6 vs. vehicle, n =15, P <0.05. Figure 5F). Meanwhile, R428 treatment

significantly decreased the rate of IA rupture compared with that of the vehicle group (13% vs. 40%, n =15, P <0.05), which was reversed by rmGas6 treatment (67% vs. 40%, n =15; P <0.05. Figure 5G). Systolic blood pressure among the groups did not show differences and increased slowly since the induction of the model (group factor, P =0.2743; time factor, P <0.0001; no interaction effect. Figure 5H). Similarly, the symptom-free survival of mice was significantly increased in the R428 treatment group (P <0.05, n =15) and decreased in the rmGas6 treatment group (P <0.05, n =15. Figure 5I).

Discussion

In this study, we found that Axl exacerbated the process of IA rupture by increasing M1 macrophage infiltration in

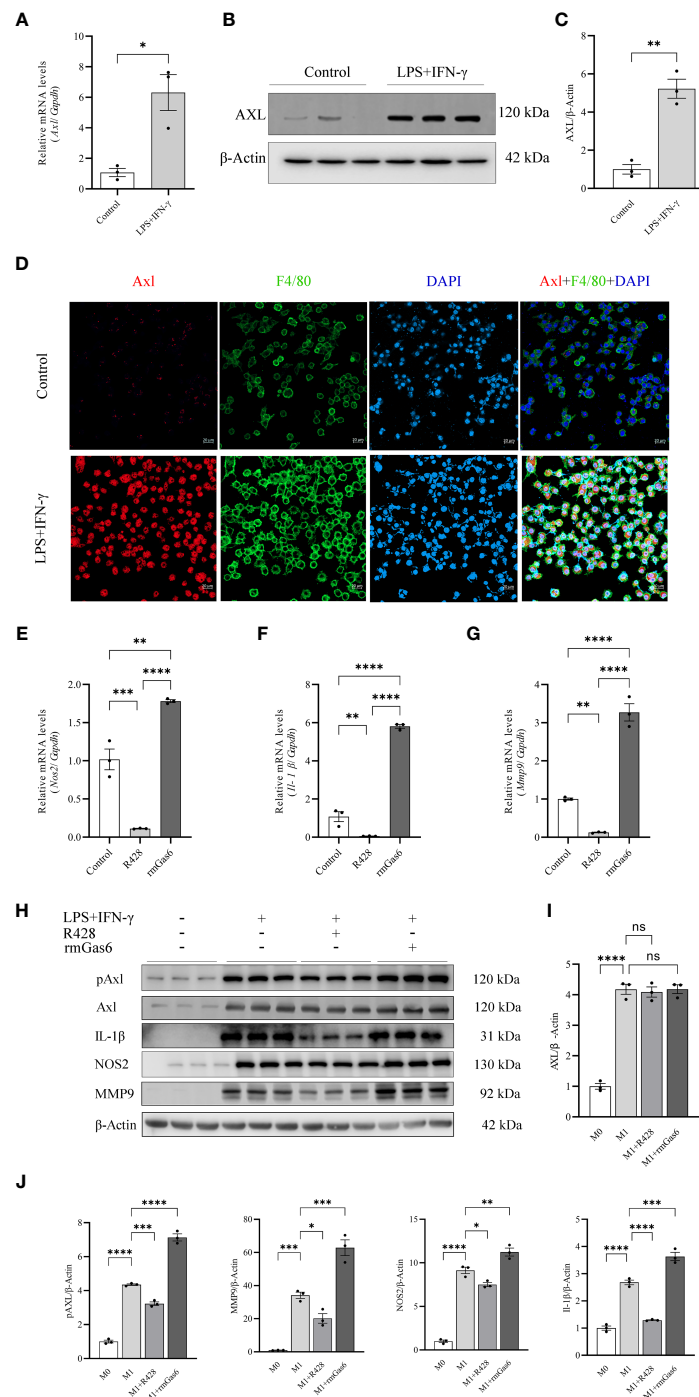


FIGURE 3
 Upregulated Axl promoted M1 macrophage polarization in BMDMs. LPS+IFN- γ increased Axl expression in BMDMs, and inhibition of Axl phosphorylation decreased the levels of inflammatory mediators in LPS+IFN- γ -induced BMDMs. LPS+IFN- γ stimulated Axl transcripts (A) and protein in BMDMs (B, C). Representative immunofluorescent images of Axl (red) expression in control and LPS+IFN- γ -stimulated BMDMs labeled with F4/80 (green) (D). qRT-PCR analysis of *IL-1 β* , *Nos2*, and *MMP9* expression in LPS+IFN- γ -induced BMDMs treated as indicated (E–G). Western blot analysis of IL-1 β , NOS2, and MMP-9 in LPS+IFN- γ -induced BMDMs treated as indicated (H–J). ns, not significant, * P <0.05, ** P < 0.01, *** P < 0.001, **** P < 0.0001.

aneurysm tissue and promoting proinflammatory responses in mice. Treatment with R428 to inhibit Axl phosphorylation significantly decreased the rate of IA rupture in mice. rmGas6 treatment promoted Axl phosphorylation and increased the rate of IA rupture. In addition, inhibition of Axl phosphorylation decreased STAT1 phosphorylation, attenuating M1 macrophage

polarization *in vivo*. Mechanistically, Axl activation enhanced the STAT1/HIF-1 α signaling pathway to promote macrophage polarization toward M1, which could be abolished by STAT1 knockdown. These findings potentially provide a new therapeutic target and may facilitate pharmacological treatment for IA.

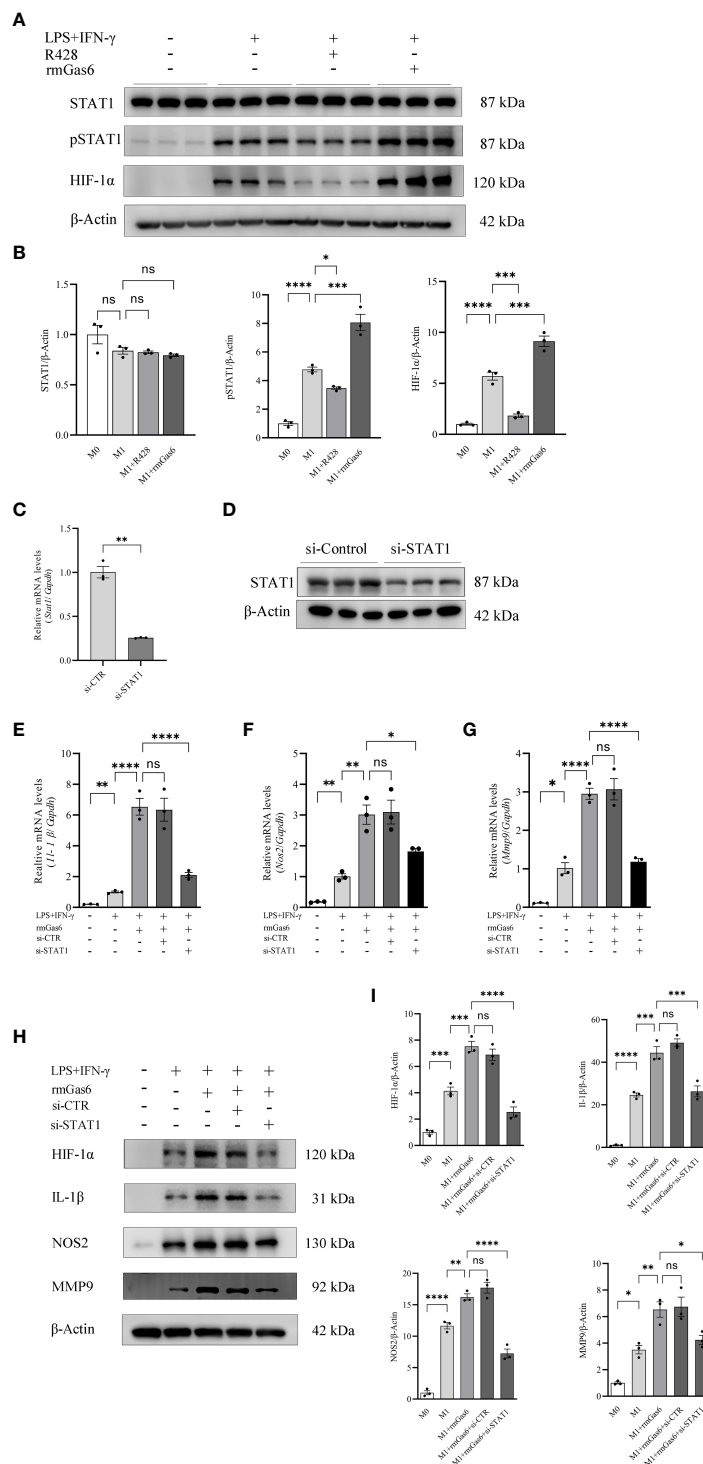


FIGURE 4
Axl skewed macrophage polarization toward M1 via STAT1/HIF-1 α activation. A. STAT1 phosphorylation and HIF-1 α activation measured by western blot 6 h after incubation with R428 or rmGas6 (A, B). Verification of the efficiency of STAT1 knockdown at the mRNA (C) and protein levels (D). The effects of STAT1 knockdown on IL-1 β , Nos2, and MMP9 secretion were measured by qRT-PCR (E–G) and western blotting in rmGas6-treated BMDMs (H, I). ns, not significant, *P<0.05, **P< 0.01, ***P< 0.001, ****P< 0.0001.

Our results showed more CD86⁺ M1 macrophages in ruptured IAs than in unruptured IAs. Additionally, R428, an Axl-specific inhibitor, significantly decreased the infiltration of M1 macrophages into the artery wall and the occurrence of IA rupture. Our findings are consistent with other studies that

suggest that macrophage polarization is associated with IA rupture. Macrophage infiltration is critical for aneurysm formation and rupture, and macrophage-mediated inflammation is a key biological pathway for IA rupture (22). Hasan et al. found an imbalance of M1/M2 macrophages and a trend toward M1

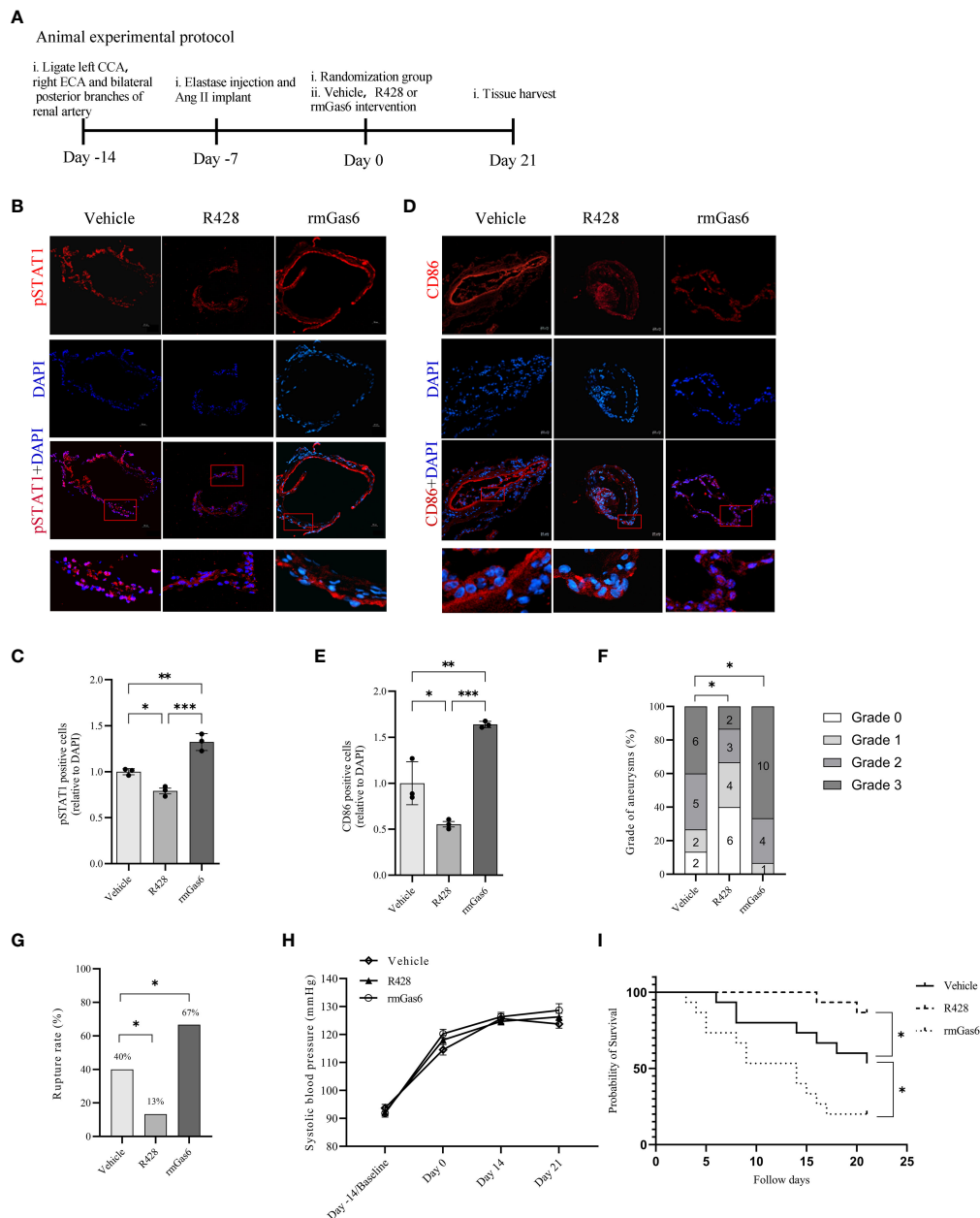


FIGURE 5

Axl promoted intracranial aneurysm progression and rupture in mouse models. (A), Animal treatment protocol. (B, C), Representative immunofluorescent images and quantitative analysis of pSTAT1 (red)-positive cells in unruptured aneurysms treated as indicated. (D, E), Representative immunofluorescent images and quantitative analysis of CD86 (red)-positive cells in unruptured aneurysms treated as indicated. Scale bar=20 μ m. (F), Grade of intracranial aneurysm progression. (G), Incidence of intracranial aneurysm rupture. (H), Systolic blood pressure between groups. (I), Symptom-free curve (log-rank analysis curve) (n=15). *P < 0.05, **P < 0.01, ***P < 0.001.

macrophages in ruptured IAs compared with unruptured IAs (10). There was a lower incidence of IA in a murine model due to macrophage depletion by clodronate liposomes and macrophage dysfunction by MCP-1 knockout (7). Macrophages infiltrate into intracranial arterial walls across endothelial cells and secrete proinflammatory cytokines and metalloproteinases (MMPs), such as MMP-2 and MMP-9, to disassemble the collagen matrix, which can lead to the destruction of the arterial wall and rupture (23).

We found that Axl expression was upregulated in unruptured IAs and further upregulated in ruptured IAs compared with normal

arteries. These results indicated that Axl is involved in IA rupture. Meanwhile, the double immunofluorescence anti-Axl and anti-F4/80 antibodies, a macrophage-specific marker, in IA sections and Axl colocalized with F4/80⁺ cells in mouse IA sections showed the relationship between Axl expression and macrophage infiltration. We also found that smooth muscle cells in mouse aneurysms expressed AXL in contrast to those in normal vessels. Okada et al. (24) have shown that BMDMs are the major source of M1 macrophage infiltration into IA regions. These findings suggest that Axl may modulate M1 macrophage infiltration into the aneurysm wall of mice.

We found that LPS/IFN- γ promoted Axl expression and phosphorylation in BMDMs and THP-1 macrophages. Axl depends on Gas6 for its activation, and Gas6 requires Axl for its stable maintenance *in vivo* (17). Endogenous Gas6 levels may influence AXL receptor activation. rmGas6 is the specific ligand for Axl activation. We also found that R428 treatment had no effect on Gas6 expression in LPS/IFN- γ -primed THP-1 cells. R428 only or R428 plus recombinant Gas6 inhibited Axl activation. These results suggested that R428 inhibited Axl phosphorylation independently of added exogenous rGas6.

Upon binding with the ligand Gas6, Axl dimerizes and becomes phosphorylated, leading to the activation of downstream mitogen-activated protein kinase (MAPK) (25–27). Both LPS and IL-4 promote Axl expression, and the activation of Axl receptors occurs in BMDMs after stimulation with LPS to activate TLR receptors (17, 28). It would be interesting to investigate whether AXL activation occurs by cross-activation with other AXL receptor units or another heterodimeric receptor in further research. BMDMs were stimulated with LPS/IFN- γ to polarize toward M1 macrophages to mimic the inflammatory responses of IA. Axl expression was significantly increased by LPS/IFN- γ and colabeled with F4/80. Axl boosting in the intracranial aneurysmal inflammation-related microenvironment might be associated with M1 macrophage polarization.

We also found an explicit effect of Axl on macrophage polarization after LPS/IFN- γ stimulation. Both qRT-PCR and Western blotting showed that R428 inhibited Axl phosphorylation and attenuated IL-1 β , NOS2, and MMP-9 in M1 macrophages. Conversely, the rmGas6 treatment had the opposite effect. These findings suggest that inhibition of Axl phosphorylation significantly attenuates M1 macrophage polarization and the production of IL-1 β , NOS2 and MMP9. Our results are consistent with those of previous studies. The activation of Axl augments the expression and secretion of proinflammatory cytokines such as IL-1 β , IL6, and TNF α in both macrophages and dendritic cells *via* the NLRP3 inflammasome and caspase-1, which can be enhanced by Gas6 and abolished by R428 (25, 28). Additionally, Axl augmented IL-1 β and IL-6 production in LPS-primed Kupffer cells (26). IL-1 β is important for the progression of intracranial aneurysms and acts as a representative cytokine secreted by M1 macrophages (27, 29). Macrophage-derived MMP-9 promotes intracranial aneurysm rupture (23). NOS2 is used to define classically activated M1 macrophages.

We found that R428 inhibited the levels of pSTAT1 and HIF-1 α in M1 macrophages, while rmGas6 boosted them. STAT1 knockdown caused the downregulation of HIF-1 α and inflammatory factors, including IL-1 β , NOS2 and MMP9. STAT1 is one of the key regulators of inflammation and is important for macrophage polarization (30). HIF-1 α positively regulates proinflammatory cytokines in response to LPS (31). These findings suggest that STAT1/HIF-1 α might mediate the promotion of M1 macrophage polarization by Axl.

Axl signaling in macrophages exacerbated inflammation of the intracranial artery wall through STAT1/HIF-1 α signaling. The effect of Axl was alleviated by STAT1 knockdown, emphasizing the key role of STAT1 in Axl signaling. Axl signaling promotes the

phosphorylation and activation of STAT1, which is an important signaling molecule for the inflammatory response (12, 32). In addition, HIF-1 α has been reported as the transcription factor of IL1 β and is stimulated by STAT1 (33, 34). Furthermore, DeBerge et al. (28) found that the effect of Axl was HIF-1 α dependent rather than NF- κ B dependent. Both STAT1 and HIF-1 α were linked to M1 macrophage activation within the M1/M2 macrophage polarization paradigm and served downstream of Axl signaling.

This study has some limitations. First, the animal model may not be sufficient to accurately depict the biological process of spontaneous IA rupture. Aneurysms were induced and did not spontaneously form in our models. Although the phenotype and presentation of aneurysm rupture mimic those of human intracranial aneurysms (35), it is difficult to definitively confirm the time course of Axl expression and M1 macrophage polarization during spontaneous IA rupture. Second, this study focused on STAT1/HIF-1 α signaling but did not explore other signaling pathways. Axl-mediated efferocytosis and autophagy play a protective role in stimulating autophagy to reduce the release of inflammasomes in the innate immune system during self-limiting inflammation (36–38). Third, human intracranial aneurysm tissues are difficult to obtain because most aneurysms are treated with endovascular coiling. Although we found that R428 treatment inhibits AXL activation in LPS/IFN- γ -primed THP-1 cells, we did not verify this in human primary M1 macrophages *in vitro* which may provide additional translational information for our work. The comprehensive effect of Axl might be complex in intracranial aneurysms. Nevertheless, we clarified the mechanism by which Axl exacerbates macrophage polarization to the M1 phenotype *via* STAT1/HIF-1 α signaling.

Conclusions

The activation of Axl played a detrimental role in the destruction of the arterial wall and the rupture of the IA and promoted M1 macrophage polarization and infiltration into the arterial wall by enhancing STAT1/HIF-1 α signaling. These findings suggest that the inhibition of Axl might be a potential strategy for the prevention of IA rupture. Axl plays an essential role in IA rupture and might be a potential therapeutic target for IAs.

Data availability statement

The original contributions presented in the study are included in the article/Supplementary Material. Further inquiries can be directed to the corresponding authors.

Ethics statement

The animal study was reviewed and approved by the Institutional Animal Care and Use Committee of Shanghai Jiaotong University.

Author contributions

Conceptualization, HY and BZ; statistical analysis, ZZ and XZ; Methodology, YH and GL. Writing original draft, YH and GL; Writing, review & editing, BZ; All authors have reviewed and approved the version of the manuscript.

Funding

This study was supported by the National Facility for Translational Medicine (Shanghai TMSK-2021-147), the Renji Hospital research project (RJTJ-QT-007), the National Natural Science Foundation of China (11972231), and the fourth batch of talent bases in Guizhou Province, China [No. (2013)15]. The funder had no role in the study design or implementation, data collection, management, analysis, or interpretation, manuscript preparation, review, approval, and the decision to submit the manuscript for publication.

References

1. Vlak MH, Algra A, Brandenburg R, Rinkel GJ. Prevalence of unruptured intracranial aneurysms, with emphasis on sex, age, comorbidity, country, and time period: a systematic review and meta-analysis. *Lancet Neurol* (2011) 10(7):626–36. doi: 10.1016/S1474-4422(11)70109-0
2. Korja M, Lehto H, Juvela S. Lifelong rupture risk of intracranial aneurysms depends on risk factors: a prospective Finnish cohort study. *Stroke* (2014) 45(7):1958–63. doi: 10.1161/STROKEAHA.114.005318
3. Claassen J, Park S. Spontaneous subarachnoid haemorrhage. *Lancet* (2022) 400(10355):846–62. doi: 10.1016/S0140-6736(22)00938-2
4. Thompson BG, Brown RD Jr., Amin-Hanjani S, Broderick JP, Cockroft KM, Connolly ES Jr., et al. Guidelines for the management of patients with unruptured intracranial aneurysms: a guideline for healthcare professionals from the American heart Association/American stroke association. *Stroke* (2015) 46(8):2368–400. doi: 10.1161/STR.0000000000000070
5. Aoki T, Nishimura M, Matsuoka T, Yamamoto K, Furuyashiki T, Kataoka H, et al. Pge(2) -Ep(2) signalling in endothelium is activated by haemodynamic stress and induces cerebral aneurysm through an amplifying loop *Via* nf-kappab. *Br J Pharmacol* (2011) 163(6):1237–49. doi: 10.1111/j.1476-5381.2011.01358.x
6. Starke RM, Chalouhi N, Jabbour PM, Tjoumakaris SI, Gonzalez LF, Rosenwasser RH, et al. Critical role of tnfr-alpha in cerebral aneurysm formation and progression to rupture. *J Neuroinflamm* (2014) 11:77. doi: 10.1186/1742-2094-11-77
7. Kanematsu Y, Kanematsu M, Kurihara C, Tada Y, Tsou TL, van Rooijen N, et al. Critical roles of macrophages in the formation of intracranial aneurysm. *Stroke* (2011) 42(1):173–8. doi: 10.1161/STROKEAHA.110.590976
8. Turjman AS, Turjman F, Edelman ER. Role of fluid dynamics and inflammation in intracranial aneurysm formation. *Circulation* (2014) 129(3):373–82. doi: 10.1161/CIRCULATIONAHA.113.001444
9. Shikata F, Shimada K, Sato H, Ikedo T, Kuwabara A, Furukawa H, et al. Potential influences of gut microbiota on the formation of intracranial aneurysm. *Hypertension* (2019) 73(2):491–6. doi: 10.1161/HYPERTENSIONAHA.118.11804
10. Hasan D, Chalouhi N, Jabbour P, Hashimoto T. Macrophage imbalance (M1 vs. M2) and upregulation of mast cells in wall of ruptured human cerebral aneurysms: preliminary results. *J Neuroinflamm* (2012) 9:222. doi: 10.1186/1742-2094-9-222
11. Ikedo T, Minami M, Kataoka H, Hayashi K, Nagata M, Fujikawa R, et al. Dipeptidyl peptidase-4 inhibitor anagliptin prevents intracranial aneurysm growth by suppressing macrophage infiltration and activation. *J Am Heart Assoc* (2017) 6(6):e004777. doi: 10.1161/JAHA.116.004777
12. Lemke G. Biology of the Tam receptors. *Cold Spring Harb Perspect Biol* (2013) 5(11):a009076. doi: 10.1101/cshperspect.a009076
13. van der Meer JH, van der Poll T, van 't Veer C. Tam Receptors, Gas6, and protein s: roles in inflammation and hemostasis. *Blood* (2014) 123(16):2460–9. doi: 10.1182/blood-2013-09-528752

Conflict of interest

The authors declare that the research was conducted in the absence of any commercial or financial relationships that could be construed as a potential conflict of interest.

Publisher's note

All claims expressed in this article are solely those of the authors and do not necessarily represent those of their affiliated organizations, or those of the publisher, the editors and the reviewers. Any product that may be evaluated in this article, or claim that may be made by its manufacturer, is not guaranteed or endorsed by the publisher.

Supplementary material

The Supplementary Material for this article can be found online at: <https://www.frontiersin.org/articles/10.3389/fimmu.2023.1158758/full#supplementary-material>

14. Zhou L, Matsushima GK. Tyro3, axl, merck receptor-mediated efferocytosis and immune regulation in the tumor environment. *Int Rev Cell Mol Biol* (2021) 361:165–210. doi: 10.1016/bs.ircmb.2021.02.002
15. Wu H, Zheng J, Xu S, Fang Y, Wu Y, Zeng J, et al. Mer regulates Microglial/Macrophage M1/M2 polarization and alleviates neuroinflammation following traumatic brain injury. *J Neuroinflamm* (2021) 18(1):2. doi: 10.1186/s12974-020-02041-7
16. Law LA, Graham DK, Di Paola J, Branchford BR. Gas6/Tam pathway signaling in hemostasis and thrombosis. *Front Med (Lausanne)* (2018) 5:137. doi: 10.3389/fmed.2018.00137
17. Zagorska A, Traves PG, Lew ED, Dransfield I, Lemke G. Diversification of Tam receptor tyrosine kinase function. *Nat Immunol* (2014) 15(10):920–8. doi: 10.1038/ni.2986
18. Xu J, Ma F, Yan W, Qiao S, Xu S, Li Y, et al. Identification of the soluble form of tyrosine kinase receptor axl as a potential biomarker for intracranial aneurysm rupture. *BMC Neurol* (2015) 15:23. doi: 10.1186/s12883-015-0282-8
19. Nuki Y, Tsou TL, Kurihara C, Kanematsu M, Kanematsu Y, Hashimoto T. Elastase-induced intracranial aneurysms in hypertensive mice. *Hypertension* (2009) 54(6):1337–44. doi: 10.1161/HYPERTENSIONAHA.109.138297
20. Hirschi KM, Tsai KYF, Davis T, Clark JC, Knowlton MN, Bikman BT, et al. Growth arrest-specific protein-6/Axl signaling induces preclampsia in ratsdagger. *Biol Reprod* (2020) 102(1):199–210. doi: 10.1093/biolre/ioz140
21. Shibata T, Makino A, Ogata R, Nakamura S, Ito T, Nagata K, et al. Respiratory syncytial virus infection exacerbates pneumococcal pneumonia *Via* Gas6/Axl-mediated macrophage polarization. *J Clin Invest* (2020) 130(6):3021–37. doi: 10.1172/JCI125505
22. Nakaoka H, Tajima A, Yoneyama T, Hosomichi K, Kasuya H, Mizutani T, et al. Gene expression profiling reveals distinct molecular signatures associated with the rupture of intracranial aneurysm. *Stroke* (2014) 45(8):2239–45. doi: 10.1161/STROKEAHA.114.005851
23. Aoki T, Kataoka H, Morimoto M, Nozaki K, Hashimoto N. Macrophage-derived matrix metalloproteinase-2 and -9 promote the progression of cerebral aneurysms in rats. *Stroke* (2007) 38(1):162–9. doi: 10.1161/01.STR.0000252129.18605.c8
24. Okada A, Koseki H, Ono I, Kayahara T, Kurita H, Miyamoto S, et al. Identification of the unique subtype of macrophages in aneurysm lesions at the growth phase. *J Stroke Cerebrovasc Dis* (2022) 31(12):106848. doi: 10.1016/j.jstrokecerebrovasdis.2022.106848
25. Van Beusecum JP, Barbaro NR, Smart CD, Patrick DM, Loperena R, Zhao S, et al. Growth arrest specific-6 and axl coordinate inflammation and hypertension. *Circ Res* (2021) 129(11):975–91. doi: 10.1161/CIRCRESAHA.121.319643
26. Tutusaus A, de Gregorio E, Cucarull B, Cristobal H, Areste C, Graupera I, et al. A functional role of Gas6/Tam in nonalcoholic steatohepatitis progression implicates axl as therapeutic target. *Cell Mol Gastroenterol Hepatol* (2020) 9(3):349–68. doi: 10.1016/j.jcmgh.2019.10.010

27. Yamaguchi T, Miyamoto T, Shikata E, Yamaguchi I, Shimada K, Yagi K, et al. Activation of the Nlrp3/Il-1beta/Mmp-9 pathway and intracranial aneurysm rupture associated with the depletion of eralpha and Sirt1 in oophorectomized rats. *J Neurosurg* (2023) 138(1):191–8. doi: 10.3171/2022.4.JNS212945
28. DeBerge M, Grinton K, Subramanian M, Wilsbacher LD, Rothlin CV, Tabas I, et al. Macrophage axl receptor tyrosine kinase inflames the heart after reperfused myocardial infarction. *J Clin Invest* (2021) 131(6). doi: 10.1172/JCI139576
29. Moriwaki T, Takagi Y, Sadamasa N, Aoki T, Nozaki K, Hashimoto N. Impaired progression of cerebral aneurysms in interleukin-1beta-Deficient mice. *Stroke* (2006) 37(3):900–5. doi: 10.1161/01.STR.0000204028.39783.d9
30. Aaronson DS, Horvath CM. A road map for those who don't know jak-stat. *Science* (2002) 296(5573):1653–5. doi: 10.1126/science.1071545
31. Palsson-McDermott EM, Curtis AM, Goel G, Lauterbach MA, Sheedy FJ, Gleeson LE, et al. Pyruvate kinase M2 regulates hif-1alpha activity and il-1beta induction and is a critical determinant of the warburg effect in lps-activated macrophages. *Cell Metab* (2015) 21(1):65–80. doi: 10.1016/j.cmet.2014.12.005
32. Zhou H, Hu L, Li J, Ruan W, Cao Y, Zhuang J, et al. Axl kinase-mediated astrocytic phagocytosis modulates outcomes of traumatic brain injury. *J Neuroinflamm* (2021) 18(1):154. doi: 10.1186/s12974-021-02201-3
33. Parra-Izquierdo I, Castanos-Mollor I, Lopez J, Gomez C, San Roman JA, Sanchez Crespo M, et al. Lipopolysaccharide and interferon-gamma team up to activate hif-1alpha Via Stat1 in normoxia and exhibit sex differences in human aortic valve interstitial cells. *Biochim Biophys Acta Mol Basis Dis* (2019) 1865(9):2168–79. doi: 10.1016/j.bbdis.2019.04.014
34. Tannahill GM, Curtis AM, Adamik J, Palsson-McDermott EM, McGettrick AF, Goel G, et al. Succinate is an inflammatory signal that induces il-1beta through hif-1alpha. *Nature* (2013) 496(7444):238–42. doi: 10.1038/nature11986
35. Tada Y, Wada K, Shimada K, Makino H, Liang EI, Murakami S, et al. Roles of hypertension in the rupture of intracranial aneurysms. *Stroke* (2014) 45(2):579–86. doi: 10.1161/STROKEAHA.113.003072
36. Vago JP, Amaral FA, van de Loo FAJ. Resolving inflammation by Tam receptor activation. *Pharmacol Ther* (2021) 227:107893. doi: 10.1016/j.pharmthera.2021.107893
37. Han J, Bae J, Choi CY, Choi SP, Kang HS, Jo EK, et al. Autophagy induced by axl receptor tyrosine kinase alleviates acute liver injury Via inhibition of Nlrp3 inflammasome activation in mice. *Autophagy* (2016) 12(12):2326–43. doi: 10.1080/15548627.2016.1235124
38. Deretic V, Levine B. Autophagy balances inflammation in innate immunity. *Autophagy* (2018) 14(2):243–51. doi: 10.1080/15548627.2017.1402992